TOP QUARK PHYSICS AT THE TEVATRON

P. BARTOŠ
Comenius University, Mlynska dolina F1
842 48 Bratislava, Slovakia

The presentation summarizes the latest top-quark-physics results determined by the Tevatron experiments. Both CDF and D0 collaborations finalize their measurements using full datasets. The obtained results of top-quark production cross-section, production asymmetry, and top-quark polarization measurements are in agreement with the Standard Model predictions. The measurements of the top-quark mass are still competitive to the LHC results.

1 Introduction

The top quark is the heaviest known elementary particle of the Standard Model (SM). At the Tevatron $p\bar{p}$ collider, top quarks were mainly produced in pairs ($t\bar{t}$) through the strong interaction processes, dominantly by quark-antiquark annihilation, which occurred in about 85% of cases. During the Run II period (2001-2011), both the CDF and D0 experiments collected event samples of integrated luminosity of approximately 10 fb^{-1} in $\sqrt{s} = 1.96$ TeV $p\bar{p}$ collisions. Results presented in this paper are obtained using the full datasets.

The large top-quark mass, m_t, leads to a very short life time, so the top quark decays before hadronization. According to the SM, the top quark decays almost exclusively into the W boson and bottom (b) quark, while the W boson decays leptonically ($l\nu$) or hadronically ($q\bar{q}$). In the measurements, only electrons and muons are considered, including electrons and muons from leptonic decays of τ leptons. Final states of the $t\bar{t}$ events are classified by decay products of W bosons. The final states with two, one, or no leptons are referred to as the dilepton, lepton+jets, and all-jets channels, respectively.

2 Top-quark pair production cross section

The measurement of the inclusive $t\bar{t}$ production cross section provides a direct test of quantum chromodynamics (QCD) as the top quark is produced at small distances ($1/m_t$) characterized by a low value of strong coupling constant $\alpha_s = 0.1$. A potential new physics can lead to a higher value of the production cross section. The basic idea of the measurement is to select events with a fingerprint of a studied $t\bar{t}$ topology, N_{obs}, determine number of non-$t\bar{t}$ events, N_{bkg}, and take into the account corrections for an acceptance, A and trigger selection and b-jet identification efficiencies, ϵ:

$$\sigma_{t\bar{t}} = \frac{N_{\text{obs}} - N_{\text{bkg}}}{A.\epsilon.L}, \tag{1}$$

where L corresponds to the integrated luminosity.

There are several measurements from both Tevatron experiments, which were combined using a best linear unbiased estimate (BLUE) method [?] with a goal of minimizing the total uncertainty[?]. The input measurements of the combination are summarized in Table **??**. The two CDF

Table 1: The $t\bar{t}$ cross-section measurements used as inputs for the Tevatron combination. The D0 dilepton and lepton+jets measurements using constrained nuisance parameters are presented in their published form indicating only their total uncertainties.

	$\sigma_{t\bar{t}}$ [pb]	L [fb^{-1}]
CDF dilepton	7.09 ± 0.49 (stat) ± 0.67 (syst)	8.8
CDF ANN lepton+jets	7.82 ± 0.38 (stat) ± 0.41 (syst)	4.6
CDF SVX lepton+jets	7.32 ± 0.36 (stat) ± 0.61 (syst)	4.6
CDF all−jets	7.21 ± 0.50 (stat) ± 1.18 ($syst$)	2.9
D0 dilepton	7.36 ± 0.85 (stat + syst)	5.4
D0 lepton+jets	7.90 ± 0.74 (stat + syst)	5.3

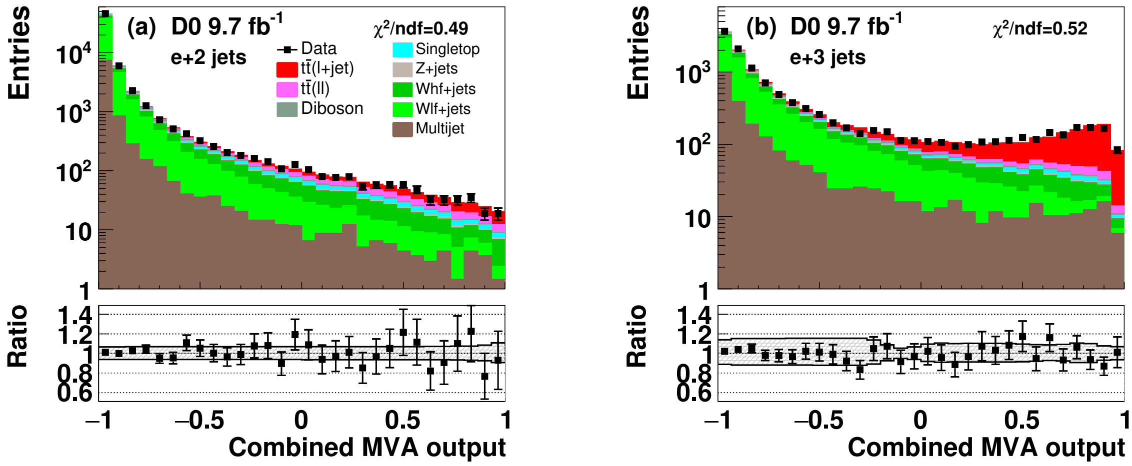

Figure 1 – Post-fit distributions of the combined MVA discriminant for e+2 jets (left), e+3 jets (right) subsamples. Statistical uncertainties of the data are shown. The post-fit systematic uncertainties are indicated by the hashed band in the bottom panel. The χ^2/ndf values take statistical and systematic uncertainties into account [?].

measurements in the lepton+jets channel apply complementary methods to discriminate signal from background. One uses an artificial neural network (ANN) to exploit differences between the kinematic properties of signal and W+jets background, without employing b-jet identification, while the second one suppresses the dominant W+jets background by reconstruction of displaced secondary vertices (SVX) to identify b jets. The combination of six measurements yields the Tevatron average of $\sigma_{t\bar{t}} = 7.60 \pm 0.20$ (stat) ± 0.29 (syst) ± 0.21 (lumi) pb, assuming $m_t = 172.5$ GeV [?]. The result is in very good agreement with fully resummed next-to-next-to-leading order (NNLO) QCD predictions of $\sigma_{t\bar{t}} = 7.35^{+0.23}_{-0.27}$ (scale + pdf) pb [?].

The D0 collaboration provides updates of both inclusive $t\bar{t}$ cross-section measurements using the full datasets [?]. In both lepton+jets and dilepton channel, a b-jet identification is based on a multivariate technique (b-ID MVA). In lepton+jets channel, the sample is divided into six subsamples by lepton type (e, μ) and jet multiplicity ($n_{\rm jet} = 2, 3, \geq 4$). To separate the signal from background, a combined MVA technique is employed. The technique inputs are selected individually for each subsample and include topological variables and various b-ID MVA discriminants. An example of output of combined MVA is shown in Figure ??. In the dilepton channel, the sample is divided into four subsamples ($e\mu$ + 1 jet, $e\mu+ \geq 2$ jets, $ee+ \geq 2$ jets, $\mu\mu+ \geq 2$ jets); the combined MVA is not used as the maximum b-ID MVA discriminant, $j^{\rm max}_{b-\rm ID}$, has provided sufficiently good separation power (Figure ??). The cross section is determined by a simultaneous fit of Monte Carlo templates to the data using systematics as nuisance parameters. The combination of the lepton+jet and dilepton channels results in cross section of $\sigma_{t\bar{t}} = 7.26 \pm 0.13$ (stat)$^{+0.57}_{-0.50}$ (syst) pb measured with relative precision of 7.6% [?]. The main sources of

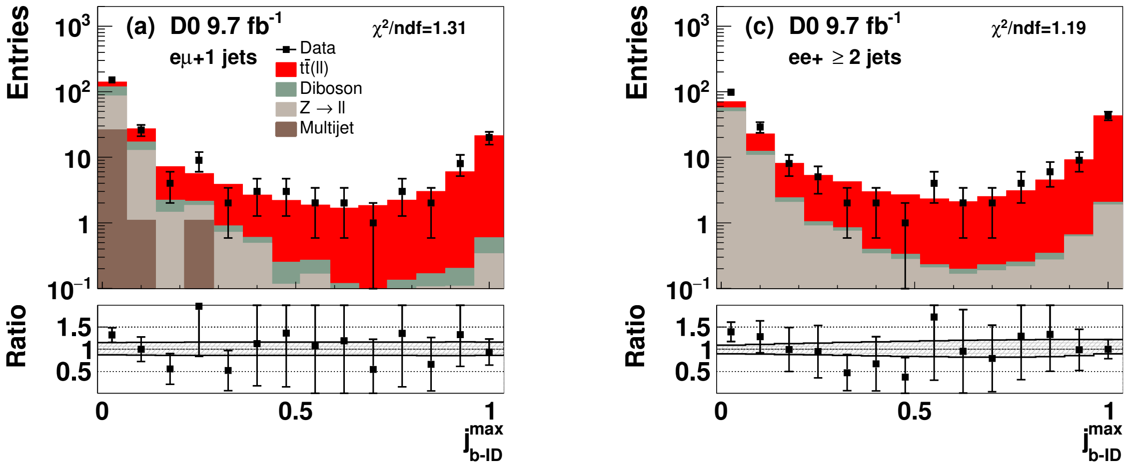

Figure 2 – The post-fit distributions of $j^{\max}_{b-\mathrm{ID}}$ for $e\mu + 1$ jet (left) and $ee+ \geq 2$ jets (right) subsamples. Statistical uncertainties of the data are shown. The post-fit systematic uncertainties are indicated by the hashed band in the bottom panel. The χ^2/ndf values take statistical and systematic uncertainties into account [?].

systematic uncertainty come from the luminosity uncertainty and hadronization. The result is in very good agreement with the SM prediction.

3 Production asymmetries

The production of $t\bar{t}$ pairs in $p\bar{p}$ collisions can result in a difference in forward and backward cross sections of top (or antitop) quarks. The forward- (backward-) produced top quarks have a positive (negative) projection of their momenta along the proton beam direction. For antitop quarks, the antiproton beam direction is taken as a reference.

In the SM, the forward-backward asymmetry is zero at the leading order (LO) in QCD. At the next-to-leading order and above, in the case of $t\bar{t}$ production via $q\bar{q}$ annihilation, positive contributions to the asymmetry come from the interference of LO and higher order diagrams, and negative contributions come from interference of initial and final state radiations. Summing over all contributions, the SM predicts positive asymmetry [?].

After the kinematic reconstruction of final $t\bar{t}$ state, one can define the forward-backward asymmetry using rapidity difference, $\Delta y = y_t - y_{\bar{t}}$:

$$A^{t\bar{t}}_{FB} = \frac{N(\Delta y > 0) - N(\Delta y < 0)}{N(\Delta y > 0) + N(\Delta y < 0)}, \tag{2}$$

where y_t ($y_{\bar{t}}$) corresponds to rapidity of top (antitop) quark. The top and antitop quarks production asymmetries lead to asymmetries in leptons from their decays. Measurement of lepton-based asymmetry does not rely on the $t\bar{t}$ final state reconstruction. An advantage is also a good lepton-charge determination and precisely measured lepton direction. The single lepton asymmetry is defined as:

$$A^{l}_{FB} = \frac{N(q_l\eta_l > 0) - N(q_l\eta_l < 0)}{N(q_l\eta_l > 0) + N(q_l\eta_l < 0)}, \tag{3}$$

where q_l and η_l correspond to the lepton electric charge sign and pseudorapidity, respectively. For dilepton channel, the dilepton asymmetry can be defined as follows:

$$A^{ll}_{FB} = \frac{N(\Delta\eta > 0) - N(\Delta\eta < 0)}{N(\Delta\eta > 0) + N(\Delta\eta < 0)}, \tag{4}$$

where $\Delta\eta$ is the pseudorapidity difference between positive and negative charged leptons.

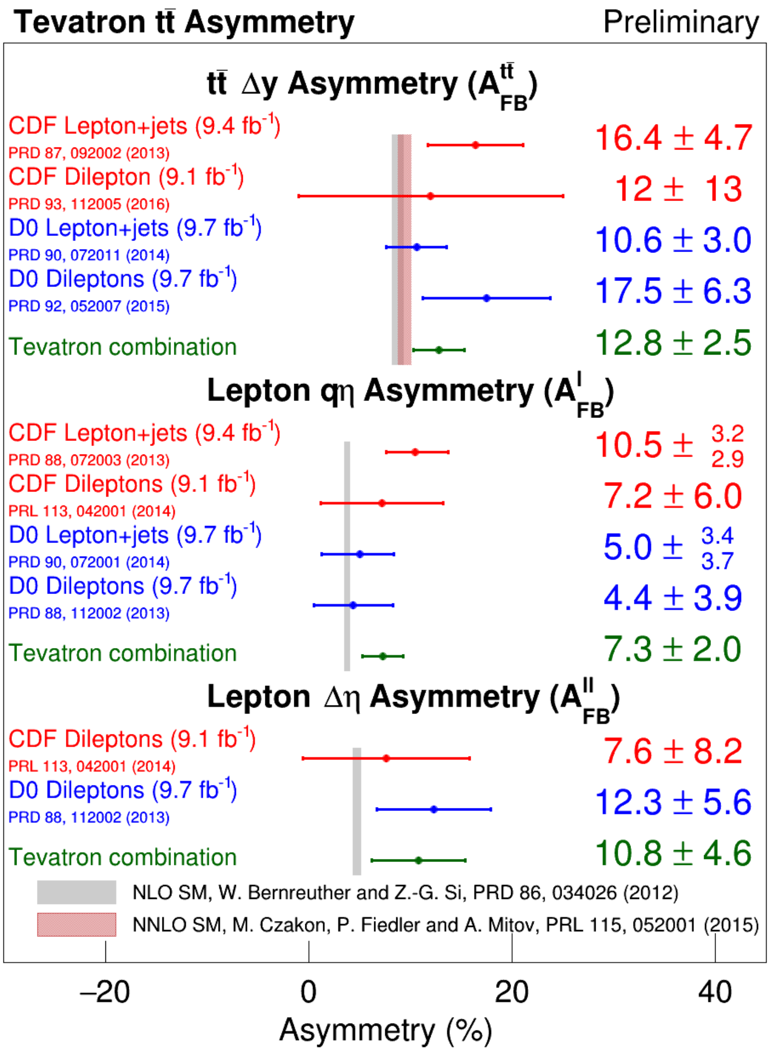

Figure 3 – Summary of inclusive top forward-backward asymmetries in $t\bar{t}$ events measured at the Tevatron [?].

The CDF and D0 collaborations combine their measurements of the inclusive asymmetries, $A^{t\bar{t}}_{FB}$, A^{l}_{FB}, and A^{ll}_{FB} using the BLUE method. Input measurements and results of combinations are shown in Figure **??**. All the inclusive asymmetries are extrapolated to the full phase space. The weights assigned to each measurement by the BLUE method are summarized in Table **??**. The three asymmetries are correlated as positive rapidity difference between top and antitop quarks is likely to result in a positive pseudorapidity difference between positive and negative charged lepton. The final measurements [?] and more refined SM predictions [?] are in agreement ($\sim 1.5\sigma$), as can be seen from Figure **??**.

Table 2: Summary of weights of each measurement contributing to the combination for three different definitions of inclusive forward-backward asymmetries.

	weight		
	$A^{t\bar{t}}_{FB}$	A^{l}_{FB}	A^{ll}_{FB}
CDF lepton+jets	0.25	0.40	–
CDF dilepton	0.01	0.11	0.32
D0 lepton+jets	0.64	0.27	–
D0 dilepton	0.11	0.23	0.68

4 Top-quark polarization

According the SM, the top quarks at the Tevatron are produced almost unpolarized. However, models beyond the SM predict enhanced polarization [?]. The top quark polarization, $P_{\hat{n}}$ can be measured in the top-quark rest frame using information of top-quark decay products, namely their angular distribution relative to some chosen axis $\hat{n}$:

$$\frac{1}{\Gamma}\frac{d\Gamma}{d\cos\theta_{i,\hat{n}}} = \frac{1}{2}(1 + P_{\hat{n}}\kappa_i \cos\theta_{i,\hat{n}}), \tag{5}$$

where i stands for decay product (lepton, quark, or neutrino), κ_i is spin-analyzing power (~ 1 for charged leptons, 0.97 for d-type quarks, -0.4 for b quarks, -0.3 for neutrinos and u-type quarks), and $\theta_{i,\hat{n}}$ is the angle between the decay-product direction and the quantization axis $\hat{n}$. The polarization is usually measured with respect to the one of the quantization axes:

- *beam axis*, given by the direction of the proton beam;
- *helicity axis*, defined by the direction of the parent top (antitop) quark;
- *transverse axis*, which is perpendicular to the production plane defined by the proton and parent top (antitop) quark directions.

The D0 collaboration provides a measurement of the top-quark polarization using the full dataset. The analysis relies on lepton+jets events requiring at least three jets and at least one jet identified as a b-jet [?]. To associate observed lepton and jets to the individual top quarks, a constrained χ^2 fit is used. In case of five or more jets in the event, only the four jets with the largest transverse momenta are assumed to originate from $t\bar{t}$ decay. In the analysis, all possible assignments of jets to the final state quarks are considered, taking into account the χ^2 and b-jet identification probabilities. To measure the polarization, a fit is performed to the reconstructed lepton angular distribution ($\cos\theta_{l,\hat{n}}$) using $t\bar{t}$ templates of $+1$ and -1 polarization (Figure **??**). The background templates are normalized to the expected event yield. The results are summarized in Table **??**. In Figure **??**, the measured longitudinal polarizations are compared with the SM predictions and several beyond SM models. The measurement along the beam axis is consistent with previous D0 measurement done in the dilepton channel [?], so the two are combined assuming 5% correlation (Table **??**, second row). The measured polarization values are consistent with the SM predictions as well as with zero polarization. The transverse polarization is measured for the first time.

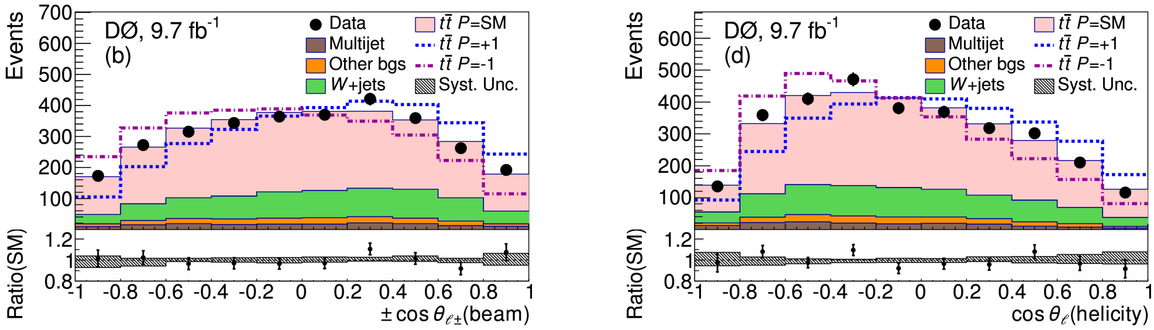

Figure 4 – Distributions of $\cos\theta_{l,\hat{n}}$ for data, expected backgrounds, and signal templates for $P = 1$, SM, $+1$ in events with at least four jets. Left (right) plot shows distribution relative to the beam (helicity) axis.

5 Top-quark pole mass

The top-quark mass, m_t, is linked to the W boson and Higgs boson masses through radiative corrections. Therefore a precise measurement of m_t provides a test of electro-weak sector of the

Table 3: Measured top-quark polarization. The combined polarization for beam axis denoted as *Beam – D0 comb.*. The total uncertainty includes statistical and systematics uncertainties.

Axis	Measured polarization	SM prediction
Beam	$+0.070 \pm 0.055$	-0.002
Beam – D0 comb.	$+0.081 \pm 0.048$	-0.002
Helicity	-0.102 ± 0.061	-0.004
Trasverse	$+0.040 \pm 0.035$	$+0.011$

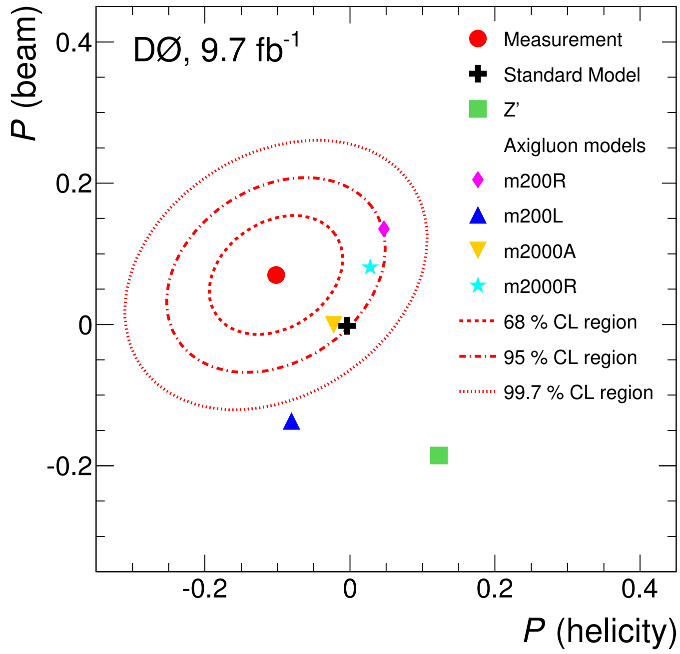

Figure 5 – The polarization measured along the beam and helicity axes in lepton+jet channel. The correlation of the two measurement uncertainties is 27%. The SM predictions and beyond SM models are shown.

SM. To increase the precision, experiments improve their techniques and provide combinations. However, the combinations are based on techniques, which use $t\bar{t}$ events simulated by Monte Carlo (MC) generators. Applying these techniques to data yields a mass quantity corresponding to the top quark mass scheme implemented in the MC. The mass quantity is referred to as the MC mass, $m_t^{\rm MC}$, and can not be used directly as an input for precise NLO/NNLO theoretical predictions. Several alternative methods can be used to measure theoretically well-defined top-quark mass (top-quark pole mass, $\overline{\rm MS}$ mass, ...). One of them employs $t\bar{t}$ production cross section to extract the top-quark pole mass, $m_t^{\rm pole}$. Theoretical arguments suggest that $m_t^{\rm MC}$ is within about 1 GeV of the $m_t^{\rm pole}$ [?].

The D0 collaboration uses the measurement of the inclusive $t\bar{t}$ production cross section mentioned in Section **??** to extract the $m_t^{\rm pole}$. The inclusive cross section is measured in eight mass points in mass range from 160 GeV to 190 GeV (Figure **??**). The experimentally measured dependence is parametrized by a four-order polynomial function. The $m_t^{\rm pole}$ is determined from a normalized joint-likelihood function, which takes into account the total experimental uncertainty, the theoretical uncertainties on the renormalization and factorization scales, and the PDF uncertainties. Employing the theory predictions at NNLO in perturbative QCD yields top-quark pole mass of 172.8 ± 1.1 (theo)$^{+3.3}_{-3.1}$ (exp) GeV with relative precision of 1.9 % [?].

The D0 collaboration provides also a measurement, which is based on extracting the $m_t^{\rm pole}$

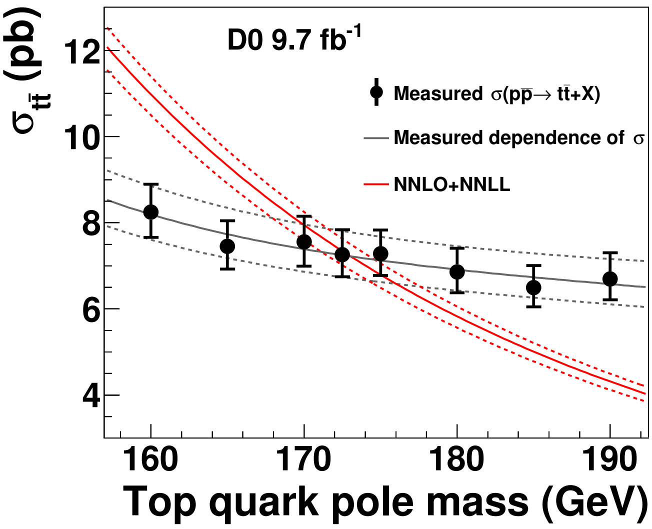

Figure 6 – The measured $t\bar{t}$ production cross section dependence on the top quark mass (points) parametrized by a quartic function (solid black line) and compared to the dependence provided by the NNLO pQCD calculation.

from a comparison of differential $t\bar{t}$ cross section predicted by perturbative QCD at NLO and NNLO with measured differential distributions [?]. Dependences of the differential cross section on the invariant mass of the $t\bar{t}$ pair, $m_{t\bar{t}}$, and on the transverse momentum of the top and antitop quarks, $p_T^{\rm top}$, are used. Data are corrected for detector effects and deconvoluted to the parton level full phase space by means of a regularized matrix-unfolding method. Figure **??** shows combined χ^2 that compares the measured differential cross sections with the theoretical calculation. In the analysis, different parton-distribution-function (PDF) sets are used in the theoretical calculations. The final result is the average $m_t^{\rm pole}$ from three glopal PDF sets (MSTW2008, CT10, and NNPDF23). At NLO the average $m_t^{\rm pole} = 167.3 \pm 2.1\ (\text{exp.}) \pm 1.5\ (\text{scale}) \pm 0.2\ (\text{PDF})$ GeV, while at NNLO $m_t^{\rm pole} = 169.1 \pm 2.2\ (\text{exp.}) \pm 0.8\ (\text{scale}) \pm 1.2\ (\text{PDF})$ GeV. These results are more precise than those based on the inclusive $t\bar{t}$ cross section measurement.

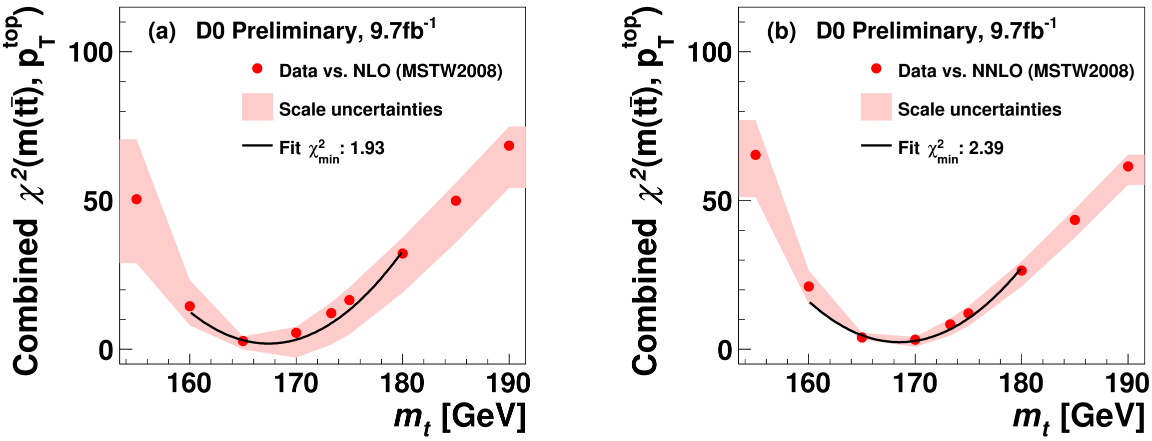

Figure 7 – The combined χ^2 distribution for the differential cross sections in terms of $m(t\bar{t})$ and $p^{\rm top}$ calculated at NLO (left) and at NNLO (right).

6 Conclusions

Tevatron experiments finalize their measurements using all collected data. The D0 collaboration has updated their measurements of the $t\bar{t}$ production cross-section measurements. The results are consistent with the Tevatron combination obtained earlier and are in very good agreement with NNLO QCD predictions. All the measurements of the top-quark production asymmetry has been finished using the full datasets. The final combinations yield inclusive production asymmetries, which are in agreement with more refined SM predictions. The D0 collaboration has provided a measurement of top-quark polarization. Obtained values are consistent with the SM expectations. The measurements of the top-quark pole mass are still competitive to the LHC results.

Acknowledgments

It is a pleasure to thank the CDF and DO collaborators for their well-done work, the top-group conveners for their help and the organizers of the Moriond EWK 2017 for a very interesting conference. This work was supported by Ministry of Education, Science, Research and Sport of the Slovak Republic.

References

1. L. Lyons, D. Gibaut, and P. Clifford, *Nucl. Instrum. Methods* A **270**, 110 (1988); A. Valassi, *Nucl. Instrum. Methods* A **500**, 391 (2003).
2. T. Aaltonen, V. M. Abazov, *et al.* (CDF and D0 Collaborations) *Phys. Rev.* D **89**, 072001 (2014).
3. P. Barnreuther, M. Czakon, and A. Mitov *Phys. Rev. Lett.* **109**, 132001 (2012).
4. V. M. Abazov *et al.* (D0 Collaboration) *Phys. Rev.* D **94**, 092004 (2016).
5. M. Czakon, P. Fiedler, and A. Mitov, *Phys. Rev. Lett.* **115**, 052001 (2015); W. Bernreuther and Z.-G. Si, *Phys. Rev.* D **86**, 034026 (2012).
6. T. Aaltonen, V. M. Abazov, *et al.* (CDF and D0 Collaborations), FERMILAB-CONF-16-386-PPD.
7. S. Fajfer, J. F. Kamenik, and B. Melic, *J. High Energy Phys.* 08 (2012) 114.
8. V. M. Abazov *et al.* (D0 Collaboration) *Phys. Rev.* D **95**, 011101(R) (2017).
9. V. M. Abazov *et al.* (D0 Collaboration), *Phys. Rev.* D **92**, 052007 (2015).
10. S. Weinzierl, Precision of the top mass, in *Proceedings of the* 50*th Rencontres de Moriond on EW Interactions and Unified Theories, La Thuile, Italy, March 14-21, 2015*, edited by E. Auge, J. Dumarchez, and J. T. T. Van (ARSIF, Paris, 2015).
11. V. M. Abazov, *et al.* (D0 Collaborations), FERMILAB-CONF-16-383-PPD.